The EMBO Journal vol.13 no.11 pp.2686–2698, 1994

Ubiquitin-assisted dissection of protein transport across membranes

Nils Johnsson and Alexander Varshavsky

Division of Biology, California Institute of Technology, Pasadena, CA 91125, USA

Communicated by A.Rich

We describe a new way to analyze targeting in protein translocation. A fusion in which ubiquitin (Ub) is positioned between a signal sequence and a reporter domain is cleaved by Ub-specific proteases (UBPs) in the cytosol unless the fusion can 'escape' into a compartment such as the endoplasmic reticulum (ER). The critical step involves rapid folding of the newly formed Ub moiety, which precludes its translocation and makes possible its cleavage by UBPs. However, if a sufficiently long spacer is present between the signal sequence and Ub, then by the time the Ub polypeptide emerges from the ribosome, the latter is already docked at the transmembrane channel, allowing the translocation of both the Ub and reporter domains of the fusion into the ER. We show that Ub fusions can be used as *in vivo* probes for kinetic and stochastic aspects of targeting in protein translocation, for distinguishing directly between cotranslational and posttranslational translocation, and for comparing the strengths of different signal sequences. This method should also be applicable to non-ER translocation.

Key words: endoplasmic reticulum/kinetics of targeting/N-end rule/*Saccharomyces cerevisiae*/signal sequence/yeast

Introduction

After emerging from ribosomes in the cytosol, proteins either remain there or are transferred to compartments separated from the cytosolic space by membranes. With a few exceptions, noncytosolic proteins begin journeys to their respective compartments by crossing membranes that enclose intracellular organelles such as the endoplasmic reticulum (ER) and mitochondria in eukaryotes or the periplasmic space in bacteria. Amino acid sequences that enable a protein to cross the membrane of a compartment are often located at the protein's N-terminus. These sequences, whose many extant names include 'signal sequences' (Blobel, 1980) and 'transferons' (Varshavsky, 1991), are targeted by translocation pathways specific for each compartment. The translocation of a protein across a compartment's membrane can start before the protein's synthesis is completed, resulting in docking of the still translating ribosome at the transmembrane channel.

The understanding of signal sequences (SSs) and translocation pathways has grown enormously over the last twenty years (reviewed by Blobel, 1980; Lee and Beckwith, 1986; Walter and Lingappa, 1986; von Heijne, 1988; Gierasch, 1989; Randall and Hardy, 1989; Rothman, 1989; Hartl and Neupert, 1990; Singer, 1990; Meyer, 1991; Wickner *et al.*, 1991; High and Dobberstein, 1992; Rapoport, 1992; Sanders and Schekman, 1992; Schatz, 1993). Nonetheless, some of the central questions about translocation remain unanswered, in part because of limitations of the existing methods. One such problem is targeting—a process whose many interacting or competing aspects include the emergence of a protein from the ribosome, the recognition of an SS-bearing nascent protein by targeting components of a translocation pathway, the folding of a nascent protein, its interactions with chaperonins, and other influences that together determine the overall rate and selectivity of the protein's translocation across the relevant membrane. Until now, analyses of kinetic aspects in translocation were limited largely to studies with isolated organelles and other cell-free systems (reviewed by Walter and Lingappa, 1986; Rapoport, 1992; but see also Andersson and von Heijne, 1991; Traxler *et al.*, 1992).

We describe a new way to analyze kinetic aspects of protein translocation. This method works *in vivo* and employs the ubiquitin (Ub) fusion technique (Bachmair *et al.*, 1986). Ub is a protein whose covalent conjugation to other proteins plays a role in a number of processes, primarily through routes that involve protein degradation (reviewed by Jentsch, 1992; Varshavsky, 1992). Unlike branched Ub–protein conjugates, which are formed posttranslationally, linear Ub adducts are formed as the translational products of natural or engineered Ub fusions (Finley *et al.*, 1989). Ub fusions are rapidly cleaved in the cytosol by Ub-specific proteases (UBPs) after the last residue (Gly76) of the Ub moiety (Baker *et al.*, 1992, and references therein).

We asked whether this latter feature of the Ub system could be used to examine temporal aspects of protein transport across the ER membrane. Our premise was as follows (Figure 1). If a Ub fusion that has been engineered to bear an N-terminal SS is cleaved in the cytosol by UBPs, the intact fusion would fail to be translocated into the ER. Conversely, if a nascent SS mediates the docking of a translating ribosome at the transmembrane channel rapidly enough, or if the fusion's Ub moiety is located sufficiently far downstream of SS, then by the time the Ub polypeptide emerges from the ribosome, the latter is already docked, and the nascent Ub moiety enters the ER before it can fold and/or be targeted by UBPs. Thus, cleavage at the Ub moiety of an SS-bearing Ub fusion in the cytosol may serve as an *in vivo* kinetic marker and a new tool for analyzing targeting in protein translocation (Figure 1). As shown below, this method is feasible, and should be generally applicable.

Results

Translocation of ubiquitin into ER

In the constructs of Figure 2, the C-terminus of mouse dihydrofolate reductase (DHFR) was extended with a

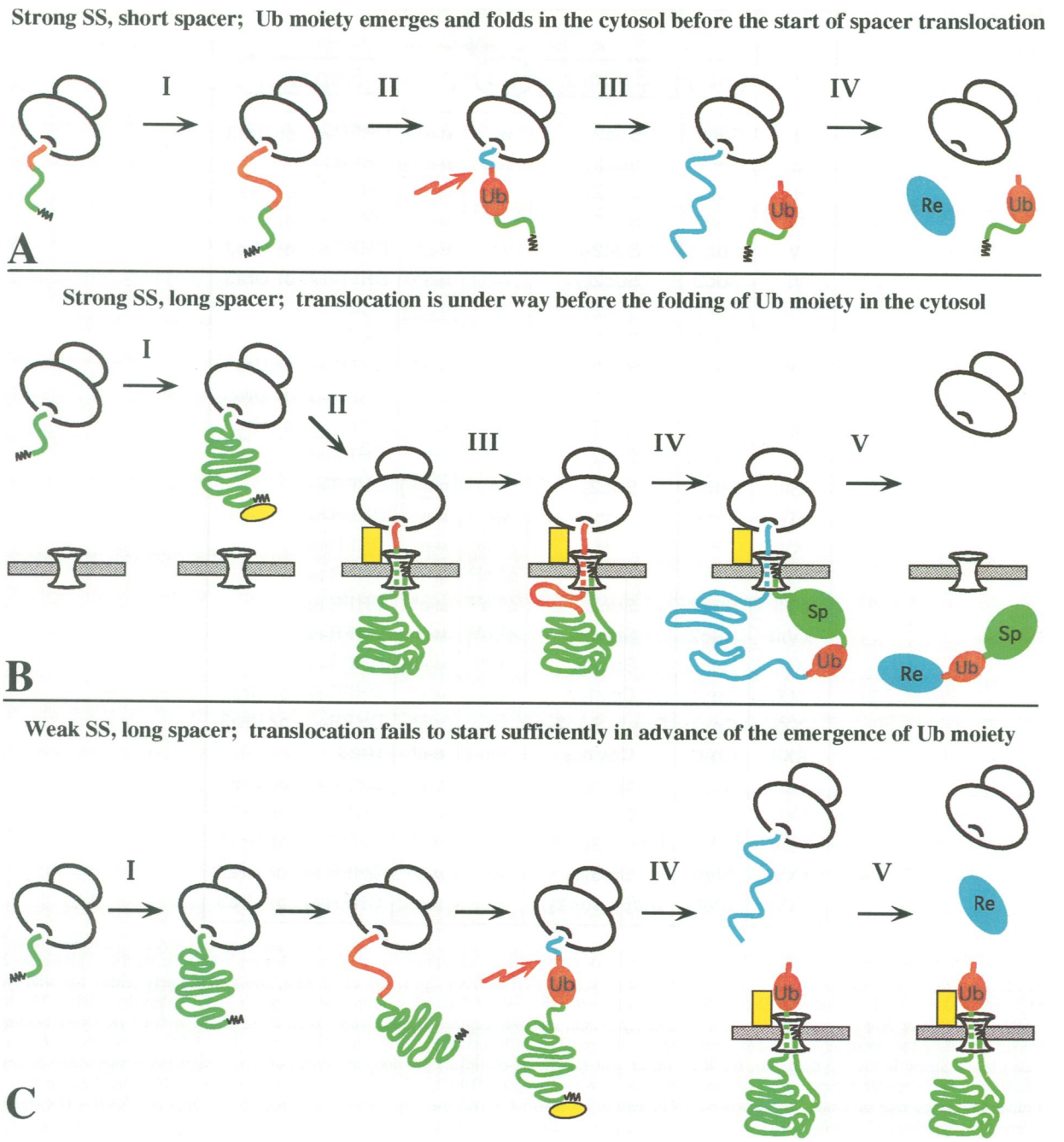

Fig. 1. Ubiquitin as a probe for targeting in protein translocation. (**A**) If a signal sequence (SS; black zigzag) is separated from the Ub moiety (red) by a sufficiently short spacer sequence (Sp; green), the Ub polypeptide emerges from the ribosome before the latter can be docked at a transmembrane channel. The rapid folding of the Ub moiety in the cytosol precludes its translocation into the endoplasmic reticulum (ER), and in addition makes Ub a target for Ub-specific proteases (UBPs), which cleave the fusion at the junction between Ub and reporter (Re; blue). (**B**) Same as in A but the spacer (Sp) sequence is now long enough for the Ub polypeptide to emerge from the ribosome after (or sufficiently shortly before) docking of the ribosome at the transmembrane channel. Under these conditions, the still unfolded Ub domain of a fusion is immediately translocated into the ER. The signal recognition particle and docking structure are denoted by yellow oval and yellow rectangle, respectively. (**C**) Same as in B but a weak SS results in a slow initiation of translocation; the Ub moiety therefore emerges from the ribosome before the latter is docked, and the Ub fusion is cleaved in the cytosol. We show that by measuring the efficiency of translocation of a full-length (uncleaved) Ub fusion as a function of the SS–Ub distance, it is possible to examine kinetic and stochastic aspects of protein translocation *in vivo*. While our results are confined to the ER, this method, termed UTA (ubiquitin translocation assay), should also be applicable to non-ER translocation.

sequence containing ha, an epitope tag derived from the influenza virus hemagglutinin, which could be recognized by a monoclonal antibody (Johnson *et al.*, 1992). To determine whether Ub, normally a cytosolic protein, could be translocated into the ER, the SS of *SUC2*-encoded invertase (SS_{suc}) of the yeast *Saccharomyces cerevisiae* and the entire 513-residue sequence of the mature Suc2 protein (Taussig and Carlson, 1983) (called Suc in the notations below) were linked to the N-terminus of Ub, whose C-terminus was extended with the DHFR-ha moiety. The resulting fusion, $SS_{suc}Suc_{518}$Ub-Mdha ['M' denotes the Met residue at the Ub–DHFR junction; 'dha' denotes DHFR-ha;

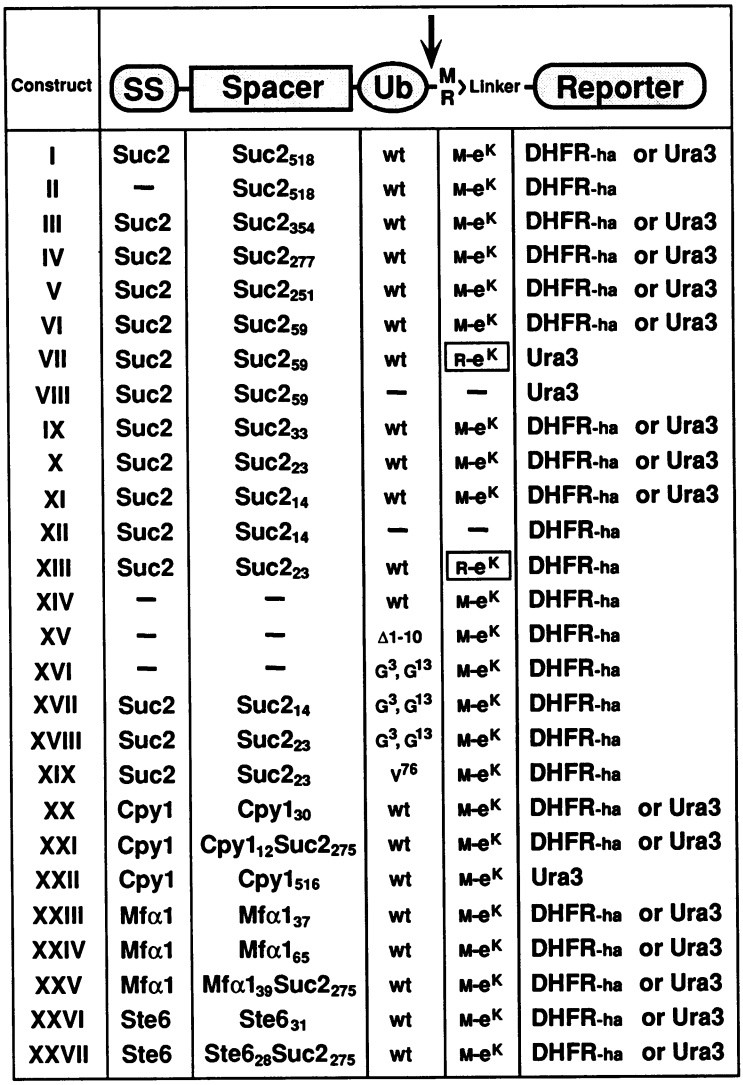

Construct						
I	Suc2	$Suc2_{518}$	wt	M-e^K	DHFR-ha	or Ura3
II	—	$Suc2_{518}$	wt	M-e^K	DHFR-ha	
III	Suc2	$Suc2_{354}$	wt	M-e^K	DHFR-ha	or Ura3
IV	Suc2	$Suc2_{277}$	wt	M-e^K	DHFR-ha	or Ura3
V	Suc2	$Suc2_{251}$	wt	M-e^K	DHFR-ha	or Ura3
VI	Suc2	$Suc2_{59}$	wt	M-e^K	DHFR-ha	or Ura3
VII	Suc2	$Suc2_{59}$	wt	R-e^K	Ura3	
VIII	Suc2	$Suc2_{59}$	—	—	Ura3	
IX	Suc2	$Suc2_{33}$	wt	M-e^K	DHFR-ha	or Ura3
X	Suc2	$Suc2_{23}$	wt	M-e^K	DHFR-ha	or Ura3
XI	Suc2	$Suc2_{14}$	wt	M-e^K	DHFR-ha	or Ura3
XII	Suc2	$Suc2_{14}$	—	—	DHFR-ha	
XIII	Suc2	$Suc2_{23}$	wt	R-e^K	DHFR-ha	
XIV	—	—	wt	M-e^K	DHFR-ha	
XV	—	—	Δ1-10	M-e^K	DHFR-ha	
XVI	—	—	G^3, G^{13}	M-e^K	DHFR-ha	
XVII	Suc2	$Suc2_{14}$	G^3, G^{13}	M-e^K	DHFR-ha	
XVIII	Suc2	$Suc2_{23}$	G^3, G^{13}	M-e^K	DHFR-ha	
XIX	Suc2	$Suc2_{23}$	V^{76}	M-e^K	DHFR-ha	
XX	Cpy1	$Cpy1_{30}$	wt	M-e^K	DHFR-ha	or Ura3
XXI	Cpy1	$Cpy1_{12}Suc2_{275}$	wt	M-e^K	DHFR-ha	or Ura3
XXII	Cpy1	$Cpy1_{516}$	wt	M-e^K	Ura3	
XXIII	Mfα1	$Mf\alpha1_{37}$	wt	M-e^K	DHFR-ha	or Ura3
XXIV	Mfα1	$Mf\alpha1_{65}$	wt	M-e^K	DHFR-ha	or Ura3
XXV	Mfα1	$Mf\alpha1_{39}Suc2_{275}$	wt	M-e^K	DHFR-ha	or Ura3
XXVI	Ste6	$Ste6_{31}$	wt	M-e^K	DHFR-ha	or Ura3
XXVII	Ste6	$Ste6_{28}Suc2_{275}$	wt	M-e^K	DHFR-ha	or Ura3

Fig. 2. Ubiquitin fusion constructs. The fusions used in the work reported here contained some of the following elements: (i) SS of either Suc2, Cpy1, MFα1 or Ste6; (ii) 'spacer'—a sequence derived from Suc2, as well as from Cpy1, MFα1 or Ste6; (iii) a Ub moiety (either the wild-type or mutant); (iv) 'linker'—a 42 residue sequence derived from residues 318–348 of *E.coli* Lac repressor (Bachmair and Varshavsky, 1989). The linker bore either Met (M) or Arg (R) residues at the Ub–linker junction, and was denoted, respectively, as M-e^K or R-e^K, with e^K [K (lysine)-containing extension] indicating the invariant 41 residue portion of the linker. When Ub fusions were cleaved in the cytosol by UBPs at the Ub–linker junction (indicated by an arrow in the top diagram), the R-e^K linker (but not the M-e^K linker) provided a reporter-attached degradation signal (the N-degron) that could be used to render a reporter protein short-lived *in vivo* (Varshavsky, 1992); (v) 'reporter', which was either DHFR-ha (bearing the C-terminal ha epitope tag) or Ura3. The absence of a moiety in a construct is indicated by a dash. In constructs V–XIII and XVII–XIX, the Suc2-derived spacer bore C-terminal deletions of varying lengths. Constructs III and IV lacked, respectively, residues 242–405 and 3–243 of mature Suc2. Constructs VI–XX and XXII–XXIV contained the sequence Gly-Gly-Ser-Ser between the spacer and the Ub moiety. Constructs I–IV, XXI, XXV and XXVII contained Gly-Gly-Ser-Ser-Thr in the same position, while construct V contained Gly-Gly-Gly-Ser-Ser-Thr, and construct XXVII contained Ser-Gly-Gly-Gly-Ser-Ser-Thr. The subscript number beside a spacer domain indicates the combined length of a linker and spacer. All constructs except I and II were expressed from the P_{CUP1} promoter in the absence of added Cu^{2+}; constructs I and II were expressed from the galactose-induced P_{GAL10} promoter in the experiments of Figure 3A and B.

five non-Suc2 residues of the Suc_{518} moiety were those of a linker sequence (Figure 2, construct I)], was expressed in *S.cerevisiae*. The cells were labeled with [^{35}S]methionine for 10 min at 30°C, followed by a chase for 0, 5 or 15 min. Cell extracts (containing both compartmentalized and cytosolic proteins) were prepared in the presence of 50 mM *N*-ethylmaleimide (NEM) to inhibit UBPs. The extracts were incubated with anti-ha antibody, and immunoprecipitates were analyzed by SDS–PAGE (Figure 3A).

$SS_{suc}Suc_{518}$Ub-Mdha (Figure 2, construct I) remained largely uncleaved at the Ub–Mdha junction; instead, the newly formed fusion was gradually cleaved within its Mdha moiety (in the ER or a post-ER compartment; see below) to yield a 20 kDa, ha-containing fragment of Mdha that accumulated during the chase (fragment 3 in Figure 3A, lanes a–c). Small amounts of the 28 kDa Mdha (fragment 2) in lanes a–c of Figure 3A were at least in part an artefact of *in vitro* cleavage at the Ub–Mdha junction that resulted from incomplete inhibition of UBPs during cell extraction and immunoprecipitation (see below). By contrast, the control fusion, Suc_{518}Ub-Mdha (Figure 2, construct II), which lacked SS_{suc}, was rapidly cleaved *in vivo* by UBPs at the Ub–Mdha junction, as expected (see Introduction): the ha-containing, 28 kDa Mdha fragment of the initial fusion

was the only detectable species even immediately after the pulse (fragment 2 in Figure 3A, lanes d–f; see below for a confirmation of the inferred identity and cytosolic location of this species).

To determine the location of species 1–3 (Figure 3A), the labeled cells were pelleted immediately before their disruption, followed by analysis of both the supernatant (secreted proteins) and the cell pellet (intracellular and cell surface-associated proteins). The 20 kDa fragment produced from $SS_{suc}Suc_{518}$Ub-Mdha (fragment 3 in Figure 3A, lanes a–c) was secreted into the medium: ^{35}S in this fragment started to appear in the medium ~5 min after the pulse, and the bulk of the labeled fragment was recovered there 15 min after the pulse (fragment 3 in Figure 3B, lanes d–f). The size of the secreted fragment 3 and its retention of the ha tag (Figure 3A and B) identified it as the product of cleavage(s) within the Mdha moiety of Suc_{518}Ub-Mdha that occurred in the ER or a post-ER compartment.

The largest ha-containing species (fragment 1) in Figure 3A and B (lanes a–c) had an apparent M_r of ~125 kDa, suggesting that it was a glycosylated derivative of the translocated 86 kDa Suc_{518}Ub-Mdha. The presence of ER-specific carbohydrates in fragment 1 was confirmed by an increase of its electrophoretic mobility after treatment with Endo H (endoglycosidase H) (Figure 3C, lanes a and b). The pulse-labeled fragment 1 was not secreted during the chase (Figure 3A and B, lanes a–c).

The 28 kDa species (fragment 4 in Figure 3B, lanes a–c), appeared to be a short-lived intracellular precursor of the extracellular 20 kDa species (fragment 3). Fragment 4 was not glycosylated, and was electrophoretically indistinguishable from the cytosolic Mdha species; however, the bulk of fragment 4 was absent from the cytosol, as could be shown by fractionation experiments, in which yeast spheroplasts were disrupted under conditions that allowed the separation of membrane-enclosed compartments from the cytosol (data not shown). The formation of fragment 4 in the ER or a post-ER compartment is consistent, among other interpretations, with the presence of Ub-specific proteases in the ER. However, this possibility is unlikely (see Discussion) in view of the slow and incomplete cleavage of the translocated Ub fusion that yielded fragment 4, in contrast to rapid cleavage of an otherwise identical but SS-lacking Ub fusion in the cytosol (Figure 3A and B). We conclude that: (i) the Ub moiety within an SS-bearing fusion can be translocated into the ER (this translocation is efficient at least for those fusions whose Ub moiety is located far downstream of a signal sequence) and (ii) a newly formed Ub fusion that differs from a translocatable fusion exclusively by the absence of a signal sequence is cleaved in the cytosol at the C-terminal residue of Ub.

Ubiquitin fusions are translocated into ER or cleaved in cytosol depending on the distance between signal sequence and ubiquitin

Derivatives of $SS_{suc}Suc_{518}$Ub-Mdha that bear C-terminal deletions in the Suc_{518} spacer (Figure 2) were expressed in *S.cerevisiae*, labeled for 6 min with [^{35}S]methionine, and assayed for the relative efficiency of their translocation into the ER. Specifically, the amount of translocated and glycosylated full-length fusion (fragment 1 in Figures 3A and B and 4) was compared with the amount of the 28 kDa

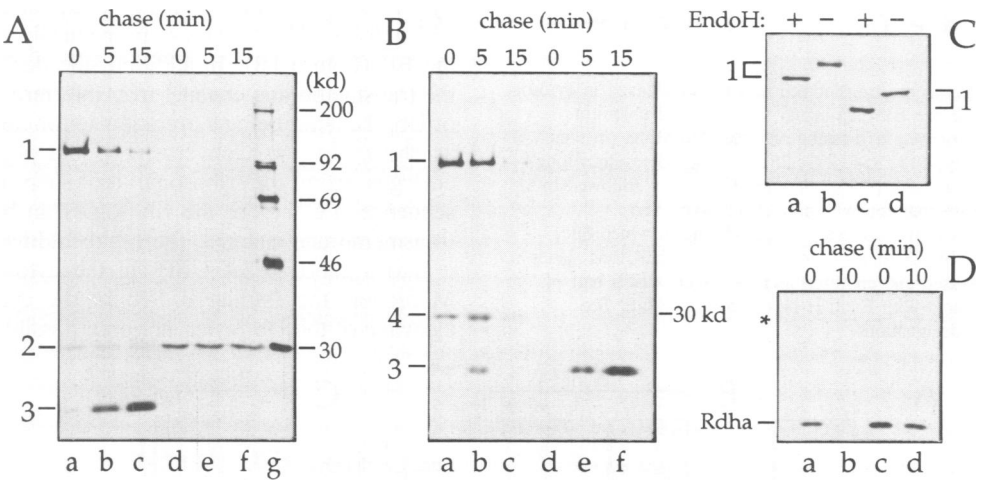

Fig. 3. *In vivo* translocation assays with ubiquitin fusions bearing signal sequences. (**A**) Lanes a–c, the metabolic fate of $SS_{suc}Suc_{518}$Ub-Mdha (Figure 2, construct I) was followed in a pulse–chase experiment, with the samples analyzed immediately (lane a), 5 (lane b) or 15 min (lane c) after a 10 min pulse with [^{35}S]methionine at 30°C. Proteins in whole-cell extracts of *S.cerevisiae* were immunoprecipitated with anti-ha antibody and analyzed by SDS–PAGE and fluorography. Lanes d–f, same as lanes a–c but with Suc_{518}Ub-Mdha (Figure 2, construct II). Lane g, molecular mass markers. Band 1: the full-length Ub fusion translocated into the ER; band 2: the 28 kDa Mdha (Met-DHFR-ha) fragment produced by cleavage of the fusion at the Ub–Mdha junction by UBPs in the cytosol; band 3: the 20 kDa, ha-containing fragment produced by cleavage of the translocated fusion within its dha moiety in the ER or a post-ER compartment. (**B**) An experiment with $SS_{suc}Suc_{518}$Ub-Mdha was carried out identically to that in A except that cells were pelleted by centrifugation immediately before their disruption, followed by SDS–PAGE analysis of proteins immunoprecipitated either from whole-cell extracts produced from cell pellets (intracellular and cell surface-associated proteins; lanes a–c) or from supernatants (secreted proteins; lanes d–f). Band 4 is a fragment of the translocated fusion that was produced by the cleavage at or near the C-terminus of Ub moiety (see the main text). (**C**) Proteins immunoprecipitated from cell extracts produced immediately after the pulse (see A) were subjected to SDS–PAGE either before (lanes b and d) or after (lanes a and c) treatment with Endo H (only the upper portion of the gel is shown). (**D**) Lanes a and b, *S.cerevisiae* expressing $SS_{suc}Suc_{23}$Ub-Rdha (Figure 2, construct XIII) were labeled with [^{35}S]methionine for 5 min, and chased for 0 or 10 min, followed by extraction, immunoprecipitation with anti-ha antibody, and SDS–PAGE. See A for the band designations. Lanes c and d, same as lanes a and b but with the congenic *ubr1*Δ strain JD15 which lacks the N-end rule pathway. An asterisk denotes an unrelated yeast protein that crossreacts wth anti-ha antibody (Johnson *et al.*, 1992).

Mdha (fragment 2 in Figure 3A), which was produced in the cytosol by cleavage at the Ub–Mdha junction. The notation 'fragment 1', initially used to denote the translocated full-length fusion Suc_{518}Ub-Mdha (Figure 3A and B, lanes a–c), was retained in Figure 4 to denote a series of progressively shorter translocated fusions that differed by the length of their invertase-derived spacer. As with the full-length fusion (Figure 2, construct I and Figure 3C, lanes a and b), treatment with Endo H was used to verify that the shorter fusions, from Suc_{354}Ub-Mdha to Suc_{23}Ub-Mdha (Figure 2, constructs III–VI and IX), also bore ER-specific carbohydrates (in addition to the C-terminal ha tag), and hence have been translocated into the ER (Figure 3C, lanes c and d; Figure 4B, lanes c–f, and data not shown).

Shortening the spacer between SS_{suc} and the Ub moiety from 518 to 251 residues did not result in a significant change of translocation efficiency (Figure 4A, lanes a–d). However, the translocation of the Ub moiety was detectably less efficient when SS_{suc} and Ub were 59 and 33 residues apart (Figure 4A, lanes e and f), and decreased dramatically when SS_{suc} and Ub were 23 residues apart (Figure 4B, lane c). The translocation of Ub was abolished when this distance was reduced to 14 residues (Figure 4B, lane a; compare with lanes c and e; note also increases in the cytosolic Mdha upon decreases in translocation among these fusions). The Mdha moieties of these fusions did not contribute to the observed inhibition of their translocation into the ER, because $SS_{suc}Suc_{14}$Mdha (Figure 2, construct XII), which lacked Ub, was translocated efficiently (Figure 5B, lanes a and b), in contrast to $SS_{suc}Suc_{14}$Ub-Mdha (Figure 2, construct XI and Figure 4B, lanes a and b).

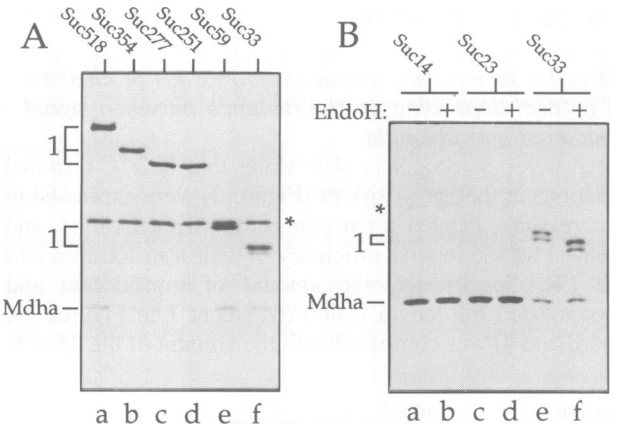

Fig. 4. Ubiquitin fusions are translocated into ER or cleaved in cytosol depending on the distance between signal sequence and ubiquitin. (**A**) Lanes a–f, *S.cerevisiae* expressing $SS_{suc}Suc_xUb$-Mdha (in which Suc_x was, respectively, 518, 354, 277, 251, 59 and 33 residues long) (Figure 2) were labeled with [^{35}S]methionine for 6 min, followed by extraction, immunoprecipitation with anti-ha antibody, and SDS–PAGE. (**B**) Endo H tests. $SS_{suc}Suc_x$Ub-Mdha in which Suc_x was 14 (lanes a and b), 23 (lanes c and d) or 33 residues long (lanes e and f), were expressed and analyzed as in A except that a half of each sample was treated with Endo H before SDS–PAGE. See Figure 3A for band designations.

We conclude that the *in vivo* translocation of an SS_{suc}-bearing Ub fusion into the ER is efficient if the Ub moiety is located ~30 or more residues from SS_{suc}. Translocation of the Ub moiety is precluded if SS_{suc} and Ub are less than ~15 residues apart. An intermediate pattern is observed for intermediate SS–Ub distances: some of the newly formed fusion molecules are translocated into the ER in their entirety, while the rest are cleaved in the cytosol at the C-terminal residue of Ub. The latter finding underscores the stochastic nature of a kinetic partitioning between two mutually exclusive fates of a nascent SS-bearing Ub fusion: the translocation of an entire fusion into the ER or the cleavage of the same fusion in the cytosol by UBPs. (Finer distinctions in this stochastic pattern are possible through the use of a metabolic marker; see below.)

These results support the model in which the emergence of the fusion's Ub moiety from a translating ribosome after (or sufficiently shortly before) the docking of the ribosome at the transmembrane channel prevents the fusion's cleavage by UBPs in the cytosol, because under these conditions the still unfolded Ub domain is immediately translocated into the ER (Figure 1B). In addition, the docking structure at the transmembrane channel may interfere with the folding of Ub, the latter being a prerequisite for cleavage by UBPs, as shown below. Conversely, if the polypeptide of Ub emerges from the ribosome too soon after the signal sequence, i.e. before the ribosome can be docked at the transmembrane channel, the rapid folding of Ub converts it into a substrate of UBPs in the cytosol (Figure 1A). Moreover, the folding of Ub in the cytosol makes the cleavage of the Ub fusion not only possible but inevitable,

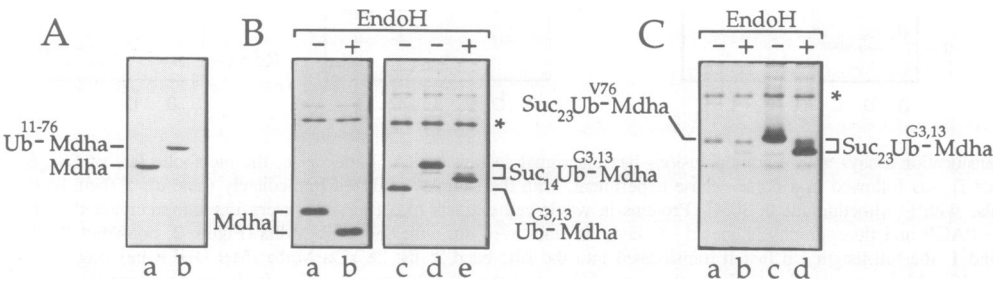

Fig. 5. Folding of ubiquitin precludes its translocation into ER and is required for recognition of ubiquitin by ubiquitin-specific proteases. (**A**) Lane a, whole-cell extracts prepared from *S.cerevisiae* that expressed Ub-Mdha (Figure 2, construct XIV) were fractionated by SDS–PAGE and probed by immunoblotting with anti-ha antibody. Lane b, same as lane a except with cells expressing Ub^{11-76}-Mdha (Figure 2, construct XV). (**B**) Lane a, *S.cerevisiae* expressing $SS_{suc}Suc_{14}$Mdha (Figure 2, construct XI) were labeled with [^{35}S]methionine for 6 min, followed by extraction, immunoprecipitation with anti-ha antibody, and SDS–PAGE. Lane b, same as lane a except that the immunoprecipitated proteins were treated with Endo H before SDS–PAGE. Lane c, same as lane a but with $Ub^{G3,13}$-Mdha (Figure 2, construct XVI). Lane d, same as lane a but with $SS_{suc}Suc_{14}Ub^{G3,13}$-Mdha (Figure 2, construct XVII). Lane e, same as lane d but after treatment with Endo H. (**C**) Lane a, same as lane a in **B** but with $SS_{suc}Suc_{23}Ub^{V76}$-Mdha (Figure 2, construct XIX). Lane b, same as lane a but after Endo H treatment. Lane c, same as lane a but with $SS_{suc}Suc_{23}Ub^{G3,13}$-Mdha (Figure 2, construct XVIII). Lane d, same as lane c but after Endo H treatment.

because the folded Ub cannot be translocated, as shown below.

Using the N-end rule pathway to verify the location and identity of DHFR-ha

The 28 kDa fragment 2 in Figure 3 was confirmed to be the product of cleavage at the Ub−Mdha junction by taking advantage of the cytosolic (non-ER) localization of the N-end rule pathway. This Ub-dependent proteolytic system targets proteins that bear destabilizing N-terminal residues (Varshavsky, 1992). Since Ub fusions are cleaved *in vivo* at the Ub−polypeptide junction irrespective of the identity of a residue at the C-terminal side of the cleavage site, they can be used to produce otherwise identical proteins bearing different (stabilizing or destabilizing) N-terminal residues (Bachmair *et al.*, 1986). The N-end rule-based degradation signal, called the N-degron, consists of a destabilizing N-terminal residue and a specific internal Lys residue (or residues) of a substrate. The Mdha moieties of our translocation substrates carried the second (lysine) determinant of the N-degron (see the legend to Figure 2) but lacked a destabilizing N-terminal residue.

To convert Mdha into an N-end rule substrate, Met (a stabilizing residue in the N-end rule) at the Ub−Mdha junction of $SS_{suc}Suc_{23}$Ub-Mdha (Figure 2, construct X) was replaced with Arg (a destabilizing residue), yielding $SS_{suc}Suc_{23}$Ub-Rdha (Figure 2, construct XIII; 'R' denotes Arg). If the latter fusion is cleaved at the Ub−Rdha junction, *and* if the cleavage takes place in the cytosol, the resulting Rdha will be a short-lived protein degraded by the N-end rule pathway (Varshavsky, 1992). Indeed, the ha-containing, 28 kDa fragment of $SS_{suc}Suc_{23}$Ub-Rdha was a short-lived protein in wild-type *S.cerevisiae* ($t_{½}$ < 10 min; Figure 3D, lanes a and b) but was long-lived in congenic *ubr1*Δ cells (Bartel *et al.*, 1990), in which the N-end rule pathway is inactive (Figure 3D, lanes c and d). These results not only confirmed the cytosolic location of fragment 2 but also showed that this fragment was produced by the cleavage immediately after Gly76 of the Ub moiety—the site of cleavage by UBPs (Baker *et al.*, 1992). The cytosolic location of Mdha produced from $SS_{suc}Suc_{23}$Ub-Mdha was independently confirmed by subcellular fractionation experiments (data not shown).

In vivo cleavage of a ubiquitin fusion requires folded ubiquitin

Does the recognition of Ub within a fusion by Ub-specific proteases require the folded conformation of Ub? In one test, we deleted the first 10 residues of the 76-residue Ub within Ub-Mdha (Figure 2, construct XV). Since these residues of Ub are part of the central β-strand in a three-stranded β-fold (Vijay-Kumar *et al.*, 1987), this deletion was expected to disrupt Ub folding. In contrast to Ub-Mdha (Figure 2, construct XIV), $Ub^{11\text{-}76}$-Mdha remained uncleaved at the $Ub^{11\text{-}76}$−Mdha junction (Figure 5A), although this junction was >60 residues away from the deleted region of Ub. In another test, the residues Ile3 and Ile13 of the Ub were replaced with Gly residues, yielding $Ub^{G3,13}$-Mdha (Figure 2, construct XVI). Since Ile3 and Ile13 are buried in the hydrophobic core of Ub (Vijay-Kumar *et al.*, 1987), this alteration was expected to decrease the conformational stability of Ub without necessarily changing its overall folding pattern. As shown in Figure 5B (lane c), $Ub^{G3,13}$-Mdha remained largely uncleaved *in vivo*, in contrast to Ub-Mdha. We conclude that the folded conformation of a fusion's Ub moiety is essential for the fusion's cleavage by UBPs.

Folding of ubiquitin precludes its translocation into ER

When Ub in the poorly translocated $SS_{suc}Suc_{23}$Ub-Mdha or in the untranslocatable $SS_{suc}Suc_{14}$Ub-Mdha (Figure 2, constructs X and XI, and Figure 4B, lanes a−d) was replaced by the conformationally destabilized $Ub^{G3,13}$, the resulting fusions (Figure 2, constructs XVII and XVIII) were efficiently translocated into the ER (Figure 5B, lanes d and e, and Figure 5C, lanes c and d). To determine directly whether the folded Ub is competent for translocation, the poorly translocated $SS_{suc}Suc_{23}$Ub-Mdha (Figure 4B, lanes c and d) was modified by replacing the last (Gly76) residue of its Ub moiety with a Val residue; this modification does not perturb the folding of Ub but precludes the cleavage of Ub^{V76} fusions by UBPs (Johnson *et al.*, 1992). If the cleavage at the Ub−Mdha junction in the cytosol were the sole reason for the near-absence of translocation of a Ub fusion such as $SS_{suc}Suc_{23}$Ub-Mdha, then its uncleavable counterpart, $SS_{suc}Suc_{23}Ub^{V76}$-Mdha (Figure 2, construct XIX), should be translocated efficiently.

Contrary to this prediction, no Endo H-produced shift in electrophoretic mobility was observed for the bulk of $SS_{suc}Suc_{23}Ub^{V76}$-Mdha, indicating that it has not been translocated into the ER (Figure 5C, lanes a and b; a minor species above the band of untranslocated $SS_{suc}Suc_{23}Ub^{V76}$-Mdha in lane a migrated faster after treatment with Endo H (lane b). The amount of ^{35}S in this band was close to that in the band of translocated $SS_{suc}Suc_{23}$Ub-Mdha in Figure 4B, lanes c and d). The apparent M_r of $SS_{suc}Suc_{23}$-Ub^{V76}-Mdha was ~2 kDa larger than that of the Endo H-treated, efficiently translocated $Suc_{23}Ub^{G3,13}$-Mdha (Figure 5C, lanes a and b; compare with lane c), suggesting that the untranslocated, cytosolic $SS_{suc}Suc_{23}Ub^{V76}$-Mdha retained its SS_{suc} signal sequence. The relative yields of immunoprecipitated (ha tag-bearing) species were much lower with the untranslocatable $SS_{suc}Suc_{23}Ub^{V76}$-Mdha than with the efficiently translocated $SS_{suc}Suc_{23}Ub^{G3,13}$-Mdha (Figure 5C, lanes a−d). Previous work (Johnson *et al.*, 1992) has shown that an uncleavable Ub moiety within a fusion can target the entire fusion for Ub-dependent degradation in the cytosol, thus providing a likely explanation for the low levels of the untranslocatable $SS_{suc}Suc_{23}Ub^{V76}$-Mdha bearing the UBP-resistant Ub moiety. We conclude that: (i) once the Ub moiety in an SS-bearing fusion folds in the cytosol, Ub cannot be translocated into the ER and (ii) the folded conformation of Ub is required for the recognition of Ub within a fusion by UBPs.

Thus, the translocation of a newly formed, SS-bearing Ub fusion into the ER can start and proceed to completion unless its Ub moiety folds in the cytosol before entering the transmembrane channel. A fusion whose Ub moiety folded before translocation is cleaved in the cytosol at the C-terminal residue of Ub. These properties of SS-bearing Ub fusions make possible their use as temporal probes for targeting in protein translocation.

Slowing of translation relaxes constraints on Ub translocation

An SS-bearing Ub fusion can be translocated into the ER only if SS and Ub are far enough apart (Figure 4); it is shown below that the minimal permitted SS−Ub distance depends

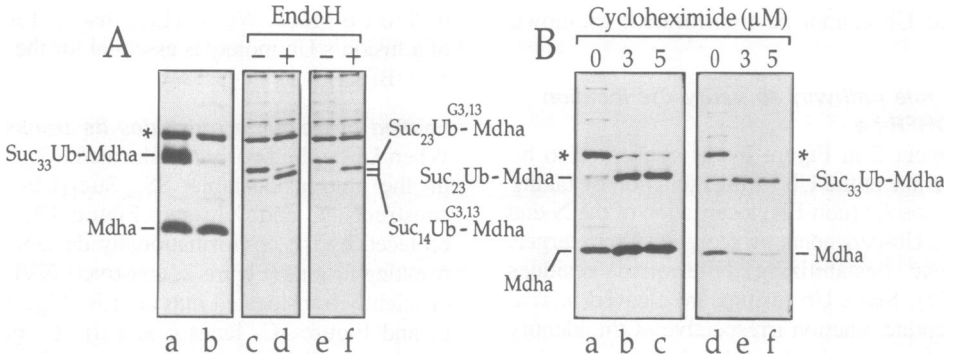

Fig. 6. Translocation of ubiquitin fusions in the absence of SRP and/or in the presence of cycloheximide. (**A**) Lane a, the wild-type (SRP-containing) YPH500 strain of *S.cerevisiae* expressing $SS_{suc}Suc_{33}$Ub-Mdha (Figure 2, construct IX) was labeled with [^{35}S]methionine for 6 min, followed by extraction, immunoprecipitation with anti-ha antibody, and SDS–PAGE. Lane b, same as lane a but with the strain BHY116 which lacks the SRP particle (see the main text). Lane c, same as lane b but with $SS_{suc}Suc_{14}Ub^{G3,13}$-Mdha (Figure 2, construct XVII). Lane d, same as lane c except that immunoprecipitated proteins were treated with Endo H before SDS–PAGE. Lane e, same as lane c but with $SS_{suc}Suc_{23}Ub^{G3,13}$-Mdha (Figure 2, construct XVIII). Lane f, same as lane e but after treatment with Endo H. (**B**) Lane a, same as lane a in A but with $SS_{suc}Suc_{23}$Ub-Mdha (Figure 2, construct X). Lanes b and c, same as lane a but in the presence of cycloheximide at 3 and 5 μg/ml, respectively. Lane d, same as lane a but with the strain BHY116 (which lacks the SRP particle) expressing $SS_{suc}Suc_{33}$Ub-Mdha (Figure 2, construct IX). Lanes e and f, same as lane d but in the presence of cycloheximide at 3 and 5 μg/ml, respectively.

on the strength of a fusion's signal sequence. The model in Figure 1 accounts for this result: it predicts that lowering the rate of translation without proportionately slowing the targeting of the signal sequence should have an effect similar to that of increasing the SS–Ub distance: in either case, it would take longer for the Ub moiety to emerge from the ribosome.

In a test of this conjecture, the translocation of $SS_{suc}Suc_{23}$Ub-Mdha (Figure 2, construct X) into the ER was monitored as described above (Figures 4 and 5) either under standard conditions or in the presence of cycloheximide (Figure 6B). In agreement with the above prediction, slowing of translation increased the translocation efficiency [defined as the ratio of translocated to untranslocated (cleaved) fusion] of $SS_{suc}Suc_{23}$Ub-Mdha from ~13% to ~32% (Figure 6B, compare lane a with lane c; at the cycloheximide concentration of 5 μM, the translation was inhibited ~10-fold). These findings further support the model of Figure 1. We note that, in contrast to the result with $SS_{suc}Suc_{23}$Ub-Mdha, the same concentration of cycloheximide did not increase the translocation efficiency of $SS_{suc}Suc_{14}$Ub-Mdha (Figure 2, construct XI), which bore a shorter spacer (data not shown).

Signal recognition particle and translocation of ubiquitin fusions

The cloning of genes that encode components of the *S.cerevisiae* signal recognition particle (SRP) made possible construction of mutants that lack SRP. These strains grow slowly and are impaired in the translocation of some but not all of the tested translocation substrates (Hann and Walter, 1991). We asked whether the elimination of SRP influences the translocation of $SS_{suc}Suc_{33}$Ub-Mdha. This fusion (Figure 2, construct IX) was chosen because the length of its Suc_{33} spacer is close to a minimal length that is compatible with efficient translocation of an SS_{suc}-bearing Ub fusion in wild-type cells (see above and Figure 4). As shown in Figure 6A (lanes a and b), the absence of SRP greatly reduced the *in vivo* translocation of $SS_{suc}Suc_{33}$Ub-Mdha. This reduction required the presence of the wild-type (folded) Ub moiety, because the absence of SRP had no effect on the translocation of $SS_{suc}Suc_{23}Ub^{G3,13}$-Mdha and at most a small effect on the translocation of $SS_{suc}Suc_{14}Ub^{G3,13}$-Mdha—the fusions with the same SS and even shorter spacers but a conformationally destabilized Ub moiety (Figure 2, constructs XVII and XVIII; also compare Figure 6A, lanes c and d, with Figure 5B, lanes d and e). The translocation-enhancing effect of a slower (cycloheximide-inhibited) translation persisted in the absence of the SRP: the relatively inefficient translocation of $SS_{suc}Suc_{33}$Ub-Mdha by an SRP-independent pathway became more efficient in the presence of cycloheximide (Figure 6B, lane d; compare with lanes e and f) (see Discussion).

Metabolic marker as a probe for targeting in protein translocation

An immunological tag in SS-bearing Ub fusions made possible the detection of relatively large differences between these proteins in their kinetics of targeting for translocation (Figures 2–5). However, the immunoprecipitation assay could not detect the much smaller differences between *efficiently* translocated fusions, in part because it proved difficult to inhibit completely the (artefactual) cleavage of Ub fusions by UBPs during cell extraction and immunoprecipitation. To address this problem, the dha (DHFR-ha) reporter domain was replaced with that of *S.cerevisiae Ura3* (Figure 2); the resulting constructs ($SS_{suc}Suc_{x}$Ub-MUra3) were expressed from a weak promoter (P_{CUP1} in the absence of added Cu^{2+}) in *ura3 S.cerevisiae*. Yeast Ura3 (orotidine-5′-phosphate decarboxylase) is a cytosolic enzyme of the uracil biosynthetic pathway that tolerates N-terminal extensions and is essential for growth in the absence of uracil (Alani and Kleckner, 1987). If Ura3 that has been translocated into the ER is unavailable for the uracil-synthesizing pathway, and if a Ura3-containing fusion is translocated efficiently, one might expect that trace amounts of the cytosolic Ura3 (derived from those few molecules of a fusion that have been translocated incompletely or not at all) would be growth-limiting for *ura3* cells in a medium lacking uracil. Earlier applications of metabolic markers addressed non-kinetic aspects of protein translocation (Manoil and Beckwith, 1986; Deshaies and Schekman, 1987;

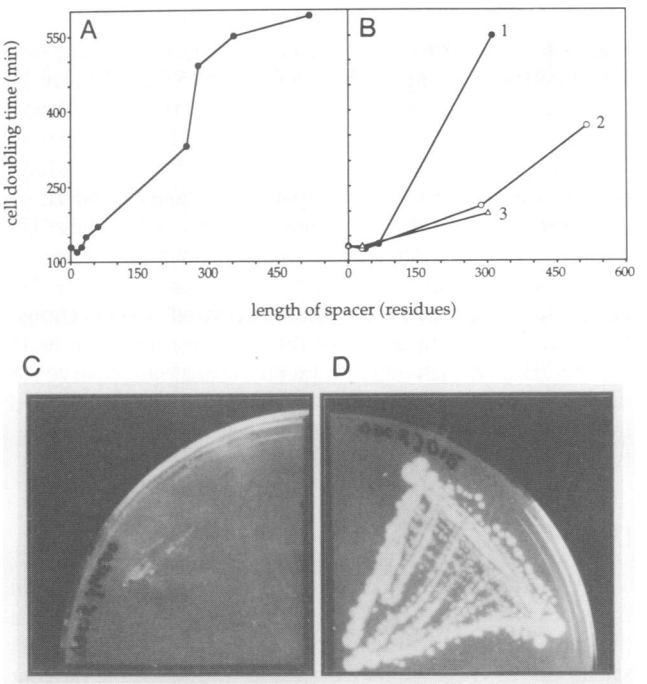

Fig. 7. Ubiquitin fusions to a metabolic marker as probes for targeting in protein translocation. (**A**) *S.cerevisiae* YPH500 were transformed with plasmids expressing $SS_{suc}Suc_xUb$-MUra3 in which the Suc_x spacer varied from 14 to 518 residues (Figure 2). The doubling times of transformants were determined in SD medium lacking uracil. (**B**) Same as in A but with *S.cerevisiae* expressing $SS_{mf\alpha}Mf\alpha_{37}Ub$-MUra3, $SS_{mf\alpha}Mf\alpha_{65}Ub$-MUra3, or $SS_{mf\alpha}Mf\alpha_{39}Suc_{275}Ub$-MUra3 (curve 1) (Figure 2, constructs XXIII–XXV); $SS_{cpy}Cpy_{30}Ub$-MUra3, $SS_{cpy}Cpy_{12}Suc_{275}Ub$-MUra3, or $SS_{cpy}Cpy_{516}Ub$-MUra3 (curve 2) (Figure 2, constructs XX-XXII); and $SS_{ste}Ste_{31}Ub$-MUra3 or $SS_{ste}Ste_{28}Suc_{275}Ub$-MUra3 (curve 3) (Figure 2, constructs XXVI and XXVII). (**C**) *S.cerevisiae* YPH500 expressing $SS_{suc}Suc_{59}Ub$-RUra3 (Figure 2, construct VII) were plated on SD medium lacking uracil, and the plates were photographed after ~3 days at 30°C. (**D**) Same as in C but with the congenic *ubr1*Δ strain JD15 that lacked the N-end rule pathway.

Sengstag *et al.*, 1990; Green and Walter, 1992; for a kinetic application, see Traxler *et al.*, 1992).

The cells that expressed $SS_{suc}Suc_{14}Ub$-MUra3 and $SS_{suc}Suc_{23}Ub$-MUra3 [whose dha-based counterparts were, respectively, untranslocatable and poorly translocated (Figure 2, constructs X and XI, and Figure 4B, lanes a–d)], had a doubling time of ~125 min at 30°C, indistinguishable from the doubling time of cells that expressed the SS-lacking Ub-MUra3 (Figure 7A and B). In the experiments with dha-based counterparts of Ura3 fusions, increasing the SS–Ub distance from 14 to 33 residues resulted in a strong increase of translocation efficiency (Figure 4B). With the corresponding Ura3 fusions, the cell doubling time increased from ~125 to ~150 min (Figure 7A), indicating that the decreasing levels of cytosolic Ura3 were becoming growth-limiting in this interval of spacer lengths. Further lengthening of the SS–Ub distance in $SS_{suc}Suc_xUb$-MUra3 resulted in progressively lower growth rates, with the cell doubling time increasing from ~125 min to ~550 min upon increase of the SS–Ub distance from 14 to 518 residues (Figure 7A). These differences among the efficiently translocated Ub fusions (Figure 7A) were not detectable using dha counterparts (Figure 4A) of the Ura3-based constructs, indicating different 'dynamic ranges' of the metabolic marker and immunoprecipitation assays.

It was the presence of Ub in the Ura3-based fusions that determined the observed levels of the cytosolic Ura3: cells that expressed $SS_{suc}Suc_{59}Ub$-MUra3 grew with a doubling time of ~170 min, whereas the same strain expressing $SS_{suc}Suc_{59}$MUra3 (which lacked the Ub moiety) had a doubling time of >550 min (Figure 2, constructs VI and VIII, Figure 7A and data not shown). Furthermore, cells expressing $SS_{suc}Suc_{59}Ub$-RUra3 (Figure 2, construct VII), in which Met (M) at the Ub–Ura3 junction had been replaced with Arg (R), a destabilizing residue in the N-end rule (Varshavsky, 1992), did not grow on uracil-free medium unless the recipient cells lacked the N-end rule pathway (Figure 7C and D). [Cells expressing an otherwise functional but short-lived Ura3 derivative such as Arg-Ura3 ($t_{½}$ < 10 min) are phenotypically Ura^- (Dohmen *et al.*, 1994).] These results, analogous to the findings with dha-based constructs (Figure 3D), confirmed that the cytosolic Ura3 was produced from SS-bearing Ub–Ura3 fusions by cleavages at the Ub–Ura3 junction, yielding either the long-lived Met-Ura3 or (in the above experiment) the short-lived Arg-Ura3.

Effects of spacer sequence

An ideal spacer would be the one whose only relevant property is length. Indeed, with the Suc2 (invertase)-derived spacer, the cell doubling time increased monotonously upon increase of the SS–Ub distance from 14 to 518 residues (Figure 7A). However, the same curve revealed significant effects of a spacer's sequence. For example, although the 277-residue, Suc2-derived spacer of the Ura3-based construct IV was only 26 residues longer than the spacer of construct V (Figure 2, constructs IV and V), the cell doubling time increased by ~150 min between constructs V and IV (Figure 7A). This nonlinear dependence between the SS–Ub distance and the cell doubling time was observed exclusively for constructs III and IV (Figure 7A). Interestingly, these Ura3-based constructs were the only ones in this series whose production involved internal deletions in Suc2 rather than C-terminal deletions used to produce the other constructs (Figure 2). One interpretation of these results (Figure 7A) is that the N-terminal portion of Suc2 is more refractory to translocation than its C-terminal portion; other possibilities include the presence of a translational pausing site in a 3′ coding portion of the *Suc2* mRNA.

The effect of a spacer's sequence (rather than of its length alone) on the efficiency of Ub translocation within a fusion makes possible the use of our assay (Figure 1) for comparisons of different spacer sequences themselves. In an extreme case, if a stop-transfer sequence is inserted upstream of Ub and C-terminally to a spacer which otherwise ensures efficient translocation of the Ub moiety into the ER, none of the resulting fusion is translocated intact, i.e. all of it is cleaved by UBPs in the cytosol (N.Johnsson and A.Varshavsky, unpublished data). It should be interesting to use this assay for comparing the influence of a stop-transfer sequence with that of related sequences that mediate translocational pausing (Chuck and Lingappa, 1992).

Targeting efficiency of a signal sequence

The apparent strengths of SSs span a wide range (Ngsee *et al.*, 1989; Kaiser and Botstein, 1990). As shown in

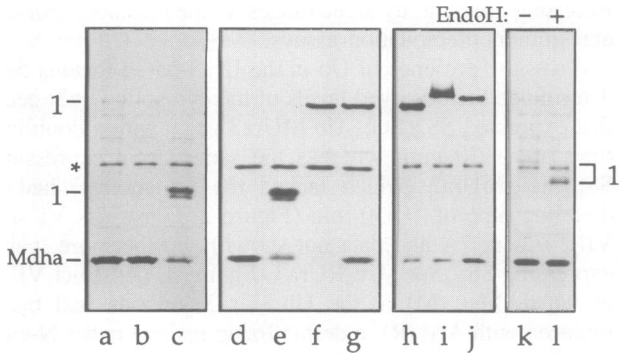

Fig. 8. Translocation of ubiquitin fusions bearing different signal sequences. *S.cerevisiae* expressing an indicated construct were labeled with [^{35}S]methionine for 6 min, followed by extraction, immunoprecipitation with anti-ha antibody, and SDS–PAGE. Lane a, $SS_{cpy}Cpy_{30}$Ub-Mdha (Figure 2, construct XX). Lane b, $SS_{mf\alpha}Mf\alpha_{37}$Ub-Mdha (Figure 2, construct XXIII). Lane c, $SS_{suc}Suc_{33}$Ub-Mdha (see also Figure 4B, lane e). Lane d, $SS_{ste}Ste_{31}$Ub-Mdha (Figure 2, construct XXVI). Lane e, same as lane c but a sample from another experiment. Lane f, $SS_{suc}Suc_{277}$Ub-Mdha (Figure 2, construct III). Lane g, $SS_{cpy}Cpy_{12}Suc_{275}$Ub-Mdha (Figure 2, construct XXI). Lane h, same as lane f but a sample from another experiment. Lane i, $SS_{mf\alpha}Mf\alpha_{39}Suc_{275}$Ubdha (Figure 2, construct XXV). Lane j, $SS_{ste}Ste_{28}Suc_{275}$Ub-Mdha (Figure 2, construct XXVII). Lane k, $SS_{mf\alpha}Mf\alpha_{65}$Ub-Mdha (Figure 2, construct XXIV). Lane l, same as lane k except that the immunoprecipitated proteins were treated with Endo H before SDS–PAGE.

Figure 8, the Ub fusion technique makes possible direct *in vivo* comparisons of different SSs. In this test, the SS of the *S.cerevisiae* Mfα1 α-factor precursor (Kurjan and Herskowitz, 1982), the SS of the Cpy1 vacuolar protease (carboxypeptidase Y) (Valls *et al.*, 1987), the SS of Suc2 (invertase), and also the first (putative) transmembrane segment of Ste6 (a transmembrane peptide transporter) (Kuchler *et al.*, 1989; McGrath and Varshavsky, 1989) were positioned upstream of Ub-Mdha. Each of these SSs was separated from the Ub moiety by a segment of a post-SS sequence of the corresponding protein (Figure 2). Strikingly, only $SS_{suc}Suc_{33}$Ub-Mdha (Figure 2, construct IX and Figure 4B, lane e) was translocated into the ER to a significant extent (Figure 8, lane c), whereas all of the newly formed $SS_{cpy}Cpy_{30}$Ub-Mdha, $SS_{mf\alpha}Mf\alpha_{37}$Ub-Mdha, and $SS_{ste}Ste_{31}$Ub-Mdha (Figure 2, constructs XX, XXIII and XXVI) were cleaved by UBPs in the cytosol (Figure 8, lanes a, b and d). It was the presence of the (folded) Ub moiety in these fusions that prevented their translocation, because otherwise identical $SS_{mf\alpha}$-bearing fusions containing the conformationally destabilized $Ub^{G3,13}$ moiety were translocated efficiently (data not shown; see Figure 5B, lane e for the analogous results with $SS_{suc}Suc_{14}Ub^{G3,13}$-Mdha).

Increased SS–Ub distances made possible the translocation of at least a fraction of a Ub fusion bearing $SS_{mf\alpha}$, SS_{cpy} or SS_{ste}. For example, $SS_{mf\alpha}Mf\alpha_{65}$Ub-Mdha (Figure 2, construct XXIV) had the region of Mfα1 from the last residue of $SS_{mf\alpha}$ to the first Kex2 cleavage site inserted between $SS_{mf\alpha}$ and Ub. While a significant fraction of this fusion was translocated into the ER, the bulk of it was still cleaved in the cytosol (Figure 8, lanes k and l). Insertion of a much longer spacer, containing also a 275-residue Suc2-derived segment, yielded $SS_{mf\alpha}Mf\alpha_{39}Suc_{275}$ Ub-Mdha, whose translocation efficiency was high and comparable to that of $SS_{suc}Suc_{277}$Ub-Mdha (Figure 2, constructs IV and XXV and Figure 8, lanes f, h and i). By contrast, the insertion of the same Suc2-derived spacer into Ub fusions bearing either SS_{cpy} or SS_{ste} (Figure 2, constructs XXI and XXVII) increased the efficiency of their translocation into the ER but not to the levels observed with $SS_{suc}Suc_{277}$Ub-Mdha and $SS_{mf\alpha}Mf\alpha_{39}Suc_{275}$Ub-Mdha (Figure 8, lanes g and j; compare with lanes f and i).

Replacements of the dha reporter with Ura3 in these Ub fusions, and measurements of the doubling time of *S.cerevisiae* as a function of the SS–Ub distance (Figure 7B) confirmed and extended the dha-based observations. Specifically, a comparison of the doubling-time curves in Figure 7B with each other and with the analogous curve for the SS_{suc}-bearing Ub–Ura3 fusions (Figure 7A) confirmed that SS_{suc} is the strongest of the four tested SSs, while $SS_{mf\alpha}$ is stronger than SS_{cpy} and SS_{ste}.

Discussion

This paper describes a new method, called UTA (ubiquitin translocation assay), which uses Ub as a kinetic probe in the context of SS-bearing Ub fusions. The temporal sensitivity of UTA stems from rapid folding of the nascent Ub polypeptide that precludes its translocation and makes it a substrate of UBPs in the cytosol shortly after the emergence of the fusion's Ub moiety from the ribosome (Figure 1).

Cotranslational and posttranslational translocation

A cotranslational process acts on a polypeptide while its C-terminus is still a peptidyl-tRNA physically associated with the translating ribosome. Thus, whether the translocation of a protein into a compartment occurs entirely post-translationally, or whether at least a C-terminus-proximal region of the protein is translocated cotranslationally is determined not only by the rate of initiation of the actual translocation of a protein across the compartment's membrane but also by the length of the protein's polypeptide chain, because a lower translocation initiation rate may be 'compensated' by a greater length of the polypeptide being made on the ribosome. One of many complexities in this kinetic landscape is 'pausing'—slowing or halting of translation that may follow the binding of SRP to an SS of a nascent protein; pausing is alleviated upon the start of translocation (Walter and Blobel, 1981; Wolin and Walter, 1989, 1993). Whether SRP-mediated pausing actually occurs *in vivo* and whether it is as tight *in vivo* as in certain (not all) cell-free translocation systems remains to be determined. Yet another complication is the existence of SRP-independent ER translocation (Hann and Walter, 1991). The understanding of these and related problems would be helped by a generally applicable *in vivo* test for cotranslational translocation.

UTA (Figure 1) provides such a test, on one assumption. Specifically, the time from the emergence of the complete, 76-residue, monomeric Ub moiety of a fusion from the ribosome to the cleavage of this fusion by UBPs is presumed to be short ($<<1$ min). Correctness of this assumption is strongly suggested not only by the conformational properties of Ub [it refolds *in vitro* from the unfolded state in <1 s (Briggs and Roder, 1992)] but also by the virtually complete deubiquitination of pulse-labeled cytosolic Ub fusions

immediately after short (1 min) *in vivo* pulses (Bachmair *et al.*, 1986; Varshavsky, 1992; data not shown). The latter evidence supports the above assumption because we showed (Figure 5) that the folded conformation of Ub is required for its recognition by UBPs.

Folding of the Ub moiety within an SS-bearing Ub fusion precludes the translocation of Ub into the ER, and is rapidly followed by the (diagnostic) Ub-specific cleavage of the fusion in the cytosol (see Results). Given these directly demonstrated constraints, the finding that a sufficiently long spacer between a signal sequence and the Ub moiety in an SS-bearing Ub fusion makes possible the translocation of the Ub moiety (and hence of the rest of the fusion) into the ER (see, for example, Figure 4; see also Figure 1B) indicates that at least the post-Ub region of this fusion is translocated cotranslationally. The bulk of $SS_{suc}Suc_{1-23}$Ub-Mdha fusion was deubiquitinated in the cytosol, in contrast to $SS_{suc}Suc_{1-59}$Ub-Mdha (Figure 4). We therefore conclude that a polypeptide bearing SS_{suc} (the strongest among tested SSs) would be translocated posttranslationally in wild-type *S.cerevisiae* at 30°C if the polypeptide contained fewer than ~150 residues. This estimate was produced by adding the length of the $SS_{suc}Suc_{1-23}$ region to the length of Ub (76 residues) and to the ~30 residues of a nascent protein that are sequestered between its tRNA-bound C-terminus and the 'exit' site in the ribosome. Conversely, the translocation of an SS_{suc}-bearing polypeptide significantly larger than ~17 kDa across the ER membrane would be expected to occur cotranslationally, i.e. it would start before the polypeptide's release from the translating ribosome. Analogous considerations, based on the results shown in Figure 8, predict that even a ~33 kDa SS-bearing polypeptide would be translocated posttranslationally under the same conditions if it contains a weaker SS such as SS_{cpy}. Given the effects of a spacer sequence (rather than of its length alone) on the translocation of Ub within a fusion (see Results), these estimates should be viewed as approximate and spacer context-dependent.

The finding that a spacer length that is sufficient for the cotranslational translocation of a Ub fusion bearing a relatively strong SS such as SS_{suc} may prove insufficient for the cotranslational translocation of an otherwise identical Ub fusion bearing a weaker SS, for example, SS_{cpy}, further supports the model in Figure 1.

SRP dependence and relative strengths of signal sequences

The absence of SRP has strikingly different consequences for the translocation efficiencies of otherwise identical fusions that contain the wild-type or conformationally destabilized Ub moieties (the latter are translocation-competent and are not recognized by UBPs) (Figure 6A). These SRP-dependent effects could not result from differences in these fusions' initial targeting for translocation, because they shared the $SS_{suc}Suc_{14}$ N-terminal region. In the absence of SRP, the emerging polypeptide of an SS-bearing Ub fusion resides in the cytosol for a longer time before the translating ribosome docks at the transmembrane channel. This delay increases the fraction of fusion molecules whose Ub folds in the cytosol, thereby precluding the fusion's translocation and causing the (diagnostic) cleavage of the fusion at its Ub moiety. We found that inefficient translocation of an SS-bearing Ub fusion in the absence of SRP can be made more efficient if the translation is made slower by cycloheximide (Figure 6). This result is consistent with the possibility that SRP increases the efficiency of targeting for translocation by either slowing or halting the translation of an SRP-bound polypeptide until the ribosome has docked.

The *SUC2*-encoded invertase is among the proteins whose translocation is at most weakly inhibited in *S.cerevisiae* mutants lacking SRP (Hann and Walter, 1991). Our results (Figures 6A and 8) suggest that this is so because even relatively large N-terminal portions of invertase that emerge from a ribosome into the cytosol do not undergo rapid aggregation or folding into a translocation-incompetent structure. By contrast, some other translocation substrates may assume translocation-incompetent conformations in the cytosol quickly enough to preclude their ER translocation in a cell with a reduced rate of targeting for translocation owing to the absence of SRP. One prediction of this model is that replacing the natural SSs of such substrates with a relatively weak SS such as SS_{cpy} should inhibit their translocation (in wild-type cells) to a much greater extent than would be observed with SS_{cpy}-bearing invertase under the same conditions. Note that Ub itself can be regarded as an example of a polypeptide whose translocation into the ER must be cotranslational in either the presence or absence of SRP; the actual constraints on Ub translocation are in fact even more stringent, because the polypeptide of Ub must not emerge from the ribosome before its docking at the transmembrane channel (Figure 1).

Earlier comparisons of the relative strengths of SSs involved a variety of assays, including those measuring the overall rate of a substrate's secretion or the rate of acquisition of ER-specific carbohydrates by a substrate (Ngsee *et al.*, 1989; Kaiser and Botstein, 1990). The UTA method greatly increases the resolution and 'dynamic range' of such comparisons (see Figure 8 and Results), in part because the parameter being determined (the minimal SS−Ub distance that allows translocation of an intact Ub fusion) is directly relevant to the targeting steps preceding translocation, can be varied in small increments, and does not require a temporal (pulse−chase) assay.

Why do signal sequences vary in strength?

A priori, the flux of a given protein from the cytosol into the ER can be controlled at the level of protein expression (RNA synthesis and translation). Therefore it is not immediately obvious why proteins that constitutively enter the ER should possess SSs of widely differing strengths. We propose that at least a fraction of this diversity is the result of selection pressures stemming from the following causes. (i) The rate of translation is roughly an order of magnitude lower than the maximal rate of ER translocation (specifically, the rate of translocation unconstrained by a coupled translation process). (ii) Newly formed SS-bearing proteins range from those that stay competent for translocation indefinitely to those that adopt translocation-incompetent conformations after a delay characteristic for each protein.

If most proteins entered the ER cotranslationally (for that, they would have to bear the strongest SSs), the translocation capacity of a cell would be under-utilized because the rate of translocation would be limited by the rate of translation. A more efficient arrangement would be to have the strongest (cotranslational translocation-promoting) SSs for proteins that adopt translocation-incompetent conformations soon after or

concurrently with their synthesis, and to lower the strengths of SSs in other SS-bearing proteins to levels that result in a delayed (posttranslational) translocation. In this view, a physiologically relevant mix of cotranslational and post-translational translocation in a given cell type evolved at least in part through a maximization of the posttranslational translocation mode (with varying, SS-specific delay times), resulting in the observed distribution of strengths among natural SSs. A prediction of this model that can be tested using UTA is that there should be a (not necessarily strict) positive correlation between the speed with which a newly formed SS-bearing protein adopts a translocation-incompetent conformation *in vivo* and the strength of the natural SS in this protein. The actual set of selection pressures which mediate coevolution of SSs and proteins containing them is obviously more complex than the one considered above; it resulted, for example, in some SSs being able to retard the folding of a downstream polypeptide (Randall and Hardy, 1989; Hardy and Randall, 1991).

Stochastic aspects of targeting in protein translocation

SS−Ub distances shorter than a certain critical distance (which depends on the efficiency of an SS) preclude the translocation of intact Ub fusions into the ER for the reasons described above and in Figure 1. However, even at the SS−Ub distances longer than the critical distance, some molecules of each fusion still failed to initiate the translocation before their cleavage by Ub-specific proteases in the cytosol (Figures 4 and 7).

These findings underscore the stochastic nature of kinetic partitioning between the two mutually exclusive fates of a nascent SS-bearing Ub fusion: the translocation of an entire fusion into the ER or the cleavage of the same fusion in the cytosol by UBPs. The metabolic marker-based UTA method is a sensitive assay for stochastic aspects of targeting in the ER translocation. For example, the initiation of (cotranslational) translocation of a Ub fusion before the emergence of its Ub moiety from the ribosome could be shown to occur with a probability detectably below unity even for the strongest of tested SSs and very long SS−Ub distances (Figure 7).

Is the ubiquitin system absent from ER?

The discussion below is confined exclusively to the ER because the existence of vacuole (lysosome)-mediated microautophagy results in a relatively nonselective delivery of the cytosol's contents to the vacuole and possibly also to compartments linked with the vacuole through vesicle-mediated transport. The amino acid sequences deduced from genes encoding the Ub precursors and the known UBPs in *S.cerevisiae* (Özkaynak *et al.*, 1987; Finley *et al.*, 1989; Baker *et al.*, 1992) do not contain N-terminal stretches that resemble SSs, suggesting that both Ub and UBPs are absent from the ER. This conjecture was strengthened by our finding that a large fraction of an SS-bearing Ub fusion stays uncleaved after its translocation into the ER, in contrast to the extremely rapid and complete deubiquitination of an otherwise identical untranslocated fusion in the cytosol. An ambiguity which has made these results, thus far, less than definitive stemmed from the detection of a protein species (termed fragment 4 in Figure 3A and B) that resulted from a cleavage of a fraction of the translocated Suc_{518}Ub-Mdha at or near the Ub−Mdha junction in either the ER or a post-ER compartment (see Results). Until the actual substrate specificity (Ub or non-Ub) and location (ER or post-ER) of a protease responsible for the slow cleavage of translocated Ub fusions is established, our findings bearing on the absence of UBPs from the ER remain less than conclusive.

Other applications

The UTA method should also be applicable to non-ER translocation pathways, including those of bacteria. Eubacteria such as *Escherichia coli* lack Ub and Ub-specific enzymes; however, the expression of a yeast UBP in *E.coli* has been shown to confer on cells the ability to deubiquitinate Ub fusions (Tobias *et al.*, 1991; Shrader *et al.*, 1993)—a sufficient condition for the applicability of UTA.

This work described applications of the UTA method to proteins which lack transmembrane segments. However, UTA should also provide the means to address still largely obscure kinetic and mechanistic aspects of biogenesis of transmembrane proteins. For example, positioning the Ub moiety at varying distances downstream of a putative internal SS in a multispanning transmembrane protein, and carrying out a UTA analogous to that in Figure 1 should yield insights about the timing of translocation reinitiation relative to the rate of translation of the rest of a transmembrane protein.

SS-bearing Ub fusions may also prove useful for importing short (less than ~30-residue) polypeptides into the ER. Such peptides are often too short-lived in the cytosol to be expressed at high steady-state levels. In the UTA method, they can be expressed downstream of the Ub moiety within SS-bearing Ub fusions (Figure 1B), whose deubiquitination by an (also imported) UBP directly in the ER would bypass the exposure of peptides to proteases in the cytosol, and would also generate peptides of predetermined lengths, bearing the desired N-terminal residues. Potential applications of such ER-generated peptides include their use as intra-ER ligands of MHC proteins in peptide-based vaccines.

Materials and methods

Strains and media

The *S.cerevisiae* strains used were YPH500 (*MATα ura3-52 lys2-801 ade2-101 trp1-Δ63 his3-Δ200 leu2-Δ1*) (Sikorski and Hieter, 1989), JD15 (the *ubr1Δ::LEU2* derivative of YPH500; a gift from Dr R.J.Dohmen), F1193 (formerly DBY2449) (*ura3-52 ade2 suc2-Δ9*) (a gift from Dr G.R.Fink), and BHY116 [*MATα trp1 lys2 his3 ura3 ade2 srp54::LYS2* (*rho*$^-$)] (Hann *et al.*, 1989) (a gift from Drs B.C.Hann and P.Walter). Yeast media were described by Baker *et al.* (1992). Transformation of *S.cerevisiae* was carried out as described by Dohmen *et al.* (1991a).

Test proteins

The final constructs (Figure 2) resided in the *CEN6*, *TRP1*-based vector pRS314 or in its *CEN6*, *URA3*-based counterpart pRS316 (Sikorski and Hieter, 1989). The constructs were expressed from the P_{CUP1} or the P_{GAL10} promoter (inserted between the *Bam*HI and *Eco*RI sites of the pRS314/16 polylinker; see the legend to Figure 2). In the Ub-coding constructs, the *S.cerevisiae UBI4*-derived Ub gene (Özkaynak *et al.*, 1987) was modified by inserting, using the Mutagene kit (Bio-Rad), a *Sal*I site immediately upstream of the start codon of the Ub ORF. As a result, the sequence Ser-Thr preceded the Met residue at the N-terminus of Ub moiety in the fusions of Figure 2. The C-terminus of Ub was extended by e^K ['K (lysine)-containing extension']—a 42 residue sequence derived from *E.coli* Lac repressor (Johnson *et al.*, 1992; Bachmair and Varshavsky, 1989). This region was followed by the mouse DHFR moiety and the ha epitope tag, as described by Johnson *et al.* (1992). Portions of the constructs that encoded Arg at the Ub−e^K junction, and the Ub^{V76} derivative of Ub (Figure 2, constructs XIII and XIX) were produced by replacing the 596 bp *Bst*XI

fragment encoding Ub-Met-e^K-DHFR-ha with the previously constructed counterparts of this fragment encoding the desired junctional residues (Johnson *et al.*, 1992; gifts from Dr E.Johnson). Portions of the construct that encoded Ub^{11-76} (Figure 2, construct XV) were produced by replacing the *SalI*–*Bst*XI fragment encompassing the start codon of the Ub ORF with an oligonucleotide containing an ATG codon instead of the wild-type codon 11 in the Ub ORF. Portions of the constructs encoding $Ub^{G3,13}$ (Figure 2, constructs XVI, XVII and XVIII) were produced by replacing the above *SalI*–*Bst*XI fragment with an otherwise identical, synthetic double-stranded (ds) oligonucleotide that contained Gly codons at positions 3 and 13 of the Ub ORF.

SUC2-, *CPY1*- and *MFα1*-derived portions of the fusions (Figure 2) were amplified from *S.cerevisiae* genomic DNA using PCR (Ausubel *et al.*, 1992) and primers containing a *Cla*I site flanking the start codons of the genes to be amplified, and a *Sal*I site (at the 3′ ends of primers) to allow in-frame ligations to the Ub ORF. The amplified DNA was digested with *Cla*I and *Sal*I, and subcloned in front of the *Sal*I site 5′ to the Ub-coding region. Sequencing of the clones isolated from PCR-produced constructs turned up an apparent missense mutation in *MFα1* that resulted in a Ser→Leu alteration at position 42 of the full-length Mfα1 precursor of α-factor [relative to the published sequence of *MFα1* (Kurjan and Herskowitz, 1982)]. However, since the same alteration was seen with *MFAα1* constructs amplified in two independent PCRs from the same *S.cerevisiae* genomic DNA (strain YPH500), it is likely that this alteration is a strain-specific polymorphism. The PCR-produced *SUC2* gene was not sequenced completely; instead, a *SUC2* clone was tested for the ability to confer the invertase activity (Goldstein and Lambert, 1975) on extracts from *SUC2*-transformed F1193 (*suc2*) cells. Sequences of the relevant regions of *SUC2*, *CPY1*, *STE6* and MFα1 were verified using the chain termination method (Ausubel *et al.*, 1992).

To produce construct IV (Figure 2), a ds oligonucleotide bearing a 5′ *Hin*dIII site and a 3′ *Bam*HI site, and encompassing the *SUC2* sequence from the *Hin*dIII site in the SS_{suc}-coding region to the codon encoding the second residue of mature Suc2, was used to replace the *Hin*dIII–*Bam*HI fragment in the DNA encoding construct I (Figure 2). To produce the Suc_{14} portion of constructs in Figure 2, the *Bam*HI–*Sal*I fragment of the DNA encoding construct IV was deleted, and the region encoding SS_{suc} was ligated to the region encoding Ub and downstream sequences using a linker encoding the first eight residues of mature Suc2. This strategy resulted in the insertion of a sequence encoding Gly-Ser between the second and third residues of mature Suc2. To produce the Suc_{354} portion of construct III (Figure 2), the *Ssp*I fragment was deleted from the DNA encoding construct I, and the ends were religated, yielding a sequence that encoded a derivative missing the residues 242–405 of mature Suc2. Constructs VI–VIII (Figure 2) were produced by ligating the *Bst*XI–*Sal*I fragment of *SUC2* to the *Sal*I site upstream of the Ub ORF, using a *Bst*XI–*Sal*I linker. DNA encoding $Mf\alpha_{39}Suc_{275}$ (Figure 2, construct XXV) was constructed from $SS_{suc}Suc_{518}$ by replacing the *Cla*I–*Bam*HI fragment of *SUC2* with the *Cla*I–*Sal*I fragment of *MFA1*, using a *Sal*I–*Bam*HI linker (encoding Gly-Gly-Ser-Ser-Gly-Gly). DNA encoding $Cpy_{12}Suc_{275}$ (Figure 2, construct XXI) was constructed by replacing the *Cla*I–*Bam*HI fragment of *SUC2* with the *Cla*I–*Xba*I fragment from construct XX, using an *Xba*I–*Bam*HI linker (encoding Asp-Gly-Gly). DNA encoding $SS_{ste}Ste_{31}$ (Figure 2, construct XXVI) was constructed by ligating the *Cla*I–*Spe*I fragment of *STE6* to the *Sal*I site upstream of the Ub ORF, using a *Spe*I–*Sal*I linker. To construct DNA encoding $SS_{ste}Ste_{28}Suc_{275}$ (Figure 2, construct XXVII), the above *Cla*I–*Spe*I fragment was ligated to the *Bam*HI–*Sal*I fragment of DNA encoding $SS_{suc}Suc_{518}$, using a *Spe*I–*Bam*HI linker (encoding Gly-Gly). A portion of the *STE6* gene used in constructs XXVI and XXVII (Figure 2) encompassed codons 1–890; it was isolated using PCR and synthetic primers designed similarly to those used for amplifying and subcloning *SUC2*. The *SUC2* portion of DNA encoding construct II was derived from the *Hin*dIII–*Sal*I fragment of DNA encoding $SS_{suc}Suc_{518}$.

To produce constructs encoding Ura3-based counterparts of DHFR fusions (Figure 2), the Ub-coding sequence in the plasmid pKM1218 (which encoded Ub-M-e^K-Ura3; a gift from Dr K.Madura) was replaced by the Ub-coding sequence containing a *Sal*I site immediately upstream of the Ub ORF. The *Sal*I fragment of the resulting construct that encoded Ub-M-e^K-Ura3 was inserted into *Xho*I/*Sal*I-cut pRS314 (Sikorski and Hieter, 1989), yielding pUbiUra314. The Ura3-based versions of constructs in Figure 2 were then produced by inserting *Eag*I–*Sal*I fragments (containing P_{CUP1} and encoding SSs and spacer sequences) of the corresponding DHFR-based constructs into *Eag*I/*Sal*I-cut pUbiUra314.

Labeling and immunoprecipitation assays

Unless stated otherwise, 10 ml cultures of *S.cerevisiae* were grown in SD medium (containing 0.1 mM $CuSO_4$) to an A_{600} of 0.8–1.5. Cells were pelleted by centrifugation at room temperature, washed once in SD lacking methionine, and resuspended in 0.5 ml of the same medium. After a 10 min incubation at 30°C, 0.15 mCi of ^{35}S-Translabel (ICN) was added, and the incubation was continued for either 5, 6 or 10 min, as indicated in the legends to figures. *N*-ethylmaleimide (NEM) (2 M in dimethylformamide) was then added to 50 mM. The cells were pelleted by centrifugation at 12 000 *g* for 30 s, resuspended in 0.4 ml of cold buffer A (1% Triton X-100, 0.15 M NaCl, 1 mM EDTA, 50 mM Na-HEPES, pH 7.5) containing protease inhibitors (Bartel *et al.*, 1990) and 50 mM NEM, and transferred to a microfuge tube containing 0.4 ml of 0.5 mm glass beads. Another 0.4 ml of the same buffer was added, and the suspension was vortexed six times at top speed for 20 s each time, with intermittent cooling on ice. The extracts were centrifuged at 12 000 *g* for 5 min, followed by immunoprecipitations with portions of supernatants containing equal amounts of acid-insoluble ^{35}S. Protein A–Sepharose (Repligen, Cambridge, MA) that had been crosslinked to the monoclonal anti-ha antibody 12CA5 (Field *et al.*, 1988; Johnson *et al.*, 1992) was used as described by Harlow and Lane (1988). The samples were incubated, with rocking, for 1 h at 4°C, followed by low-speed centrifugation. The pellets were washed three times with 0.8 ml of buffer A plus 0.1% SDS, and once with 20 mM Tris–HCl (pH 6.8), then resuspended in SDS-containing electrophoretic sample buffer, heated at 100°C for 3 min and centrifuged at 12 000 *g* for 30 s. The supernatants were subjected to SDS–PAGE (12%), followed by fluorography with Enhance (New England Nuclear). Where indicated the ^{35}S patterns were detected and quantified using a PhosphorImager (Molecular Dynamics).

Pulse–chase analysis was carried out as described by Dohmen *et al.* (1991b) and Johnson *et al.* (1992). Labeling cells in the presence of cycloheximide (see Figure 6B) was carried out as described above, except that before labeling for 6 min with ^{35}S-Translabel, the cells were preincubated for 10 min in growth medium containing the indicated amounts of cycloheximide, and then for another 10 min in the labeling medium (lacking methionine), also in the presence of cycloheximide. The inhibition of translation by cycloheximide was measured by determining total CCl_3COOH-insoluble ^{35}S during the labeling.

Other techniques

Growth curves. *S.cerevisiae* were grown at 30°C to an A_{600} of ~1 in SD medium containing uracil. A sample was pelleted by centrifugation at 12 000 *g* for 30 s, and resuspended in 5 ml of the same medium without uracil to yield the starting A_{600} of ~0.05. Subsequent growth of the culture was monitored using a Klett colorimeter.

Treatments with Endo H. These were carried out as described by Orlean *et al.* (1991). Before SDS–PAGE, the samples were concentrated using the CH_3OH-$CHCl_3$ procedure of Wessel and Flügge (1984).

Immunoblotting. Proteins fractionated by SDS–PAGE were electroblotted onto nitrocellulose membranes (Schleicher and Schuell). Membranes were blocked with 5% bovine serum albumin (Sigma) in phosphate-buffered saline, and then treated with anti-ha antibody and alkaline phosphatase-conjugated secondary antibody (Promega) (Harlow and Lane, 1988).

Acknowledgements

We thank the colleagues whose names are cited in the paper for their gifts of reagents, and members of this laboratory, especially E.Johnson, G.Turner, C.Byrd, J.Dohmen, F.Lévy, K.Madura and I.Ota for comments on the manuscript. N.J. is grateful to B.Bartel, J.Dohmen and E.Johnson for their friendly assistance with learning the tricks of molecular biology and yeast genetics. This work was supported by grants to A.V. from the NIH (GM31530 and DK39520). N.J. was supported by a postdoctoral fellowship from the Deutsche Forschungsgemeinschaft.

References

Alani,E. and Kleckner,N. (1987) *Genetics*, **117**, 5–12.

Andersson,H. and von Heijne,G. (1991) *Proc. Natl Acad. Sci. USA*, **88**, 9751–9754.

Ausubel,F.M., Brent,R., Moore,D.D., Seidman,J.G., Smith,J.A. and Struhl,K. (1992) *Current Protocols in Molecular Biology*. Wiley-Interscience, New York.

Bachmair,A., Finley,D. and Varshavsky,A. (1986) *Science*, **234**, 179–186.

Baker,R.T., Tobias,J.W. and Varshavsky,A. (1992) *J. Biol. Chem.*, **267**, 23364–23375.

Bartel,B., Wünning,I. and Varshavsky,A. (1990) *EMBO J.*, **9**, 3179–3189.

Blobel,G. (1980) *Proc. Natl Acad. Sci. USA*, **77**, 1496–1500.

Briggs,M.S. and Roder,H. (1992) *Proc. Natl Acad. Sci. USA*, **89**, 2017–2021.
Chuck,S.L. and Lingappa,V.R. (1992) *Cell*, **68**, 9–21.
Deshaies,R.J. and Schekman,R. (1987) *J. Cell Biol.*, **105**, 633–645.
Dohmen,R.J., Strasser,A.W.M., Höner,C.B. and Hollenberg,C.P. (1991a) *Yeast*, **7**, 691–692.
Dohmen,R.J., Madura,M., Bartel,B. and Varshavsky,A. (1991b) *Proc. Natl Acad. Sci. USA*, **88**, 7351–7355.
Dohmen,R.J., Wu,P. and Varshavsky,A. (1994) *Science*, **263**, 1273–1275.
Field,J., Nikawa,J.-I., Broek,D., McDonald,B., Rodgers,L., Wilson,I.A., Lerner,R.A. and Wigler,M. (1988) *Mol. Cell. Biol.*, **8**, 2159–2165.
Finley,D., Bartel,B. and Varshavsky,A. (1989) *Nature*, **338**, 394–401.
Gierasch,L.M. (1989) *Biochemistry*, **28**, 923–930.
Goldstein,A. and Lambert,J.O. (1975) *Methods Enzymol.*, **42**, 504–511.
Green,N. and Walter,P. (1992) *Mol. Cell. Biol.*, **12**, 276–282.
Hann,B.C. and Walter,P. (1991) *Cell*, **67**, 131–143.
Hann,B.C., Poritz,M.A. and Walter,P. (1989) *J. Cell Biol.*, **109**, 3223–3230.
Hardy,S.J.S. and Randall,L.L. (1991) *Science*, **251**, 439–443.
Harlow,E. and Lane,D. (1988) *Antibodies*. Cold Spring Harbor Laboratory Press, Cold Spring Harbor, NY.
Hartl,F.-U. and Neupert,W. (1990) *Science*, **247**, 930–938.
High,S. and Dobberstein,B. (1992) In W.Neupert and R.Lill (eds), *Membrane Biogenesis and Protein Targeting*. Elsevier, Amsterdam, pp. 105–118.
Jentsch,S. (1992) *Annu. Rev. Genet.*, **26**, 179–207.
Johnson,E.S., Bartel,B., Seufert,W. and Varshavsky,A. (1992) *EMBO J.*, **11**, 497–505.
Kaiser,C.A. and Botstein,D. (1990) *Mol. Cell. Biol.*, **10**, 3163–3173.
Kuchler,K., Sterne,R.E. and Thorner,J. (1989) *EMBO J.*, **8**, 3973–3982.
Kurjan,J. and Herskowitz,I. (1982) *Cell*, **30**, 933–943.
Lee,C. and Beckwith,J. (1986) *Annu. Rev. Cell Biol.*, **2**, 315–336.
Manoil,C. and Beckwith,J. (1986) *Science*, **233**, 1403–1408.
McGrath,J.P. and Varshavsky,A. (1989) *Nature*, **340**, 400–404.
Meyer,D.I. (1991) *Trends Cell Biol.*, **1**, 154–158.
Ngsee,J.K., Hansen,W., Walter,P. and Smith,M. (1989) *Mol. Cell. Biol.*, **9**, 3400–3410.
Orlean,P., Kuranda,M.J. and Albright,C.F. (1991) *Methods Enzymol.*, **194**, 682–696.
Özkaynak,E., Finley,D., Solomon,M.J. and Varshavsky,A. (1987) *EMBO J.*, **6**, 1429–1440.
Randall,L.L. and Hardy,S.J.S. (1989) *Science*, **243**, 1156–1159.
Rapoport,T.A. (1992) *Science*, **258**, 931–936.
Rothman,J.E. (1989) *Cell*, **59**, 591–601.
Sanders,S.L. and Schekman,R. (1992) *J. Biol. Chem.*, **267**, 13971–13974.
Schatz,G. (1993) *Protein Sci.*, **2**, 141–146.
Sengstang,C., Stirling,C., Scheckman,R. and Rine,J. (1990) *Mol. Cell. Biol.*, **10**, 672–680.
Shrader,T.E., Tobias,J.W. and Varshavsky,A. (1993) *J. Bacteriol.*, **175**, 4364–4374.
Sikorski,R.S. and Hieter,P. (1989) *Genetics*, **122**, 19–27.
Singer,S.J. (1990) *Annu. Rev. Cell Biol.*, **6**, 247–296.
Taussig,R. and Carlson,M. (1983) *Nucleic Acids Res.*, **11**, 1943–1954.
Tobias,J.W., Shrader,T.E., Rocap,G. and Varshavsky,A. (1991) *Science*, **254**, 1374–1377.
Traxler,B., Lee,C., Boyd,D. and Beckwith,J. (1992) *J. Biol. Chem.*, **267**, 5339–5345.
Valls,L.A., Hunter,C.P., Rothman,J.H. and Stevens,T.H. (1987) *Cell*, **48**, 887–897.
Varshavsky,A. (1991) *Cell*, **64**, 13–15.
Varshavsky,A. (1992) *Cell*, **69**, 725–735.
Vijay-Kumar,S., Bugg,C.E. and Cook,W.J. (1987) *J. Mol. Biol.*, **194**, 531–544.
von Heijne,G. (1988) *Biochim. Biophys. Acta*, **947**, 307–333.
Walter,P. and Blobel,G. (1981) *J. Cell Biol.*, **91**, 557–561.
Walter,P. and Lingappa,V.R. (1986) *Annu. Rev. Cell Biol.*, **2**, 499–516.
Wessel,D. and Flügge,U.I. (1984) *Anal. Biochem.*, **138**, 141–143.
Wickner,W., Driessen,A.J.M. and Hartl,F.-U. (1991) *Annu. Rev. Biochem.*, **60**, 101–124.
Wolin,S.L. and Walter,P. (1989) *J. Cell Biol.*, **109**, 2617–2622.
Wolin,S.L. and Walter,P. (1993) *J. Cell Biol.*, **121**, 1211–1219.

Received on December 31, 1993; revised on March 14, 1994